Modeling the process of liquid nitrogen outflow through a conical nozzle into vacuum chamber

© R.Kh. Bolotnova[1], V.A. Korobchinskaya[1,2], E.F. Gainullina[1,2]

[1] Mavlyutov Institute of Mechanics UFRC RAS, Ufa, Russia
[2] Ufa University of Science and Technology, Ufa, Russia
E-mail: buzina_lera@mail.ru

Received May 12, 2023
Revised October, 13, 2023
Accepted October, 30, 2023

The evolution of a liquid nitrogen jet boiling in the region of cryogenic temperatures at various initial degrees of superheat is investigated on the basis of a spatial axisymmetric two-phase model of a vapor-liquid mixture in two-temperature, single-pressure, single-velocity approximations, taking into account nonequilibrium evaporation and condensation processes. The reliability of a developed numerical method is estimated by comparison with the experimental data. The influence of the degree of superheat on the opening angle of the jet, the formation and development of vortex zones during the transition from the bubble flow mode to the vapor-droplet one with an assessment of the monodispersity level of the vapor-drop flow is analyzed.

Keywords: liquid nitrogen, conical nozzle, boiling jet, cryogenic temperatures.

DOI: 10.61011/TPL.2023.12.57601.107A

The study of the processes of formation of expanding jets of cryogenic liquids during spraying from a thin nozzle into a low-pressure vessel has an important scientific and practical significance in connection with the development and creation of devices initiating the processes of formation of liquids spraying modes in relation to various technological processes of modern power engineering, in particular, rocket technology.

The results of experimental studies of jet flows using nitrogen as a working fluid are presented in the paper [1], where the effect of increasing the degree of superheating on the evolution of spraying of a jet of boiling liquid nitrogen at cryogenic temperatures is analyzed. The velocity and droplet diameter distributions of highly superheated boiling liquid nitrogen sprays with constant injection conditions were measured. In [2,3] the results of a numerical study of critical flow phenomena of boiling vapor-water jets are presented.

The present work continues the studies based on [2,3] begun in [4], in which the evolution of a forming boiling jet of cryogenic liquid nitrogen during sudden depressurization of a high-pressure chamber into a vacuum atmosphere under conditions, close to the experiments [1], at different initial degrees of superheating $R_p = p_s(T_{inj})/p_c$ (p_s — saturation pressure for temperature T_{inj}, p_c — back pressure).

In the [1] experiments under consideration, liquid nitrogen at pressure $p_{inj} = 4$ bar and temperature $T_{inj} = 82.5$ K was in a cylindrical high-pressure vessel of length $x_h = 136$ mm and radius $y_h = 34$ mm, corresponding to volume $V_h \approx 0.5$ l, at the initial moment of time. As a result of diaphragm rupture, explosive discharge of boiling nitrogen is initiated through a conical injector nozzle of length $x_s = 30$ mm with an outlet diameter $D_{inj} = 1$ mm ($y_s = 0.5$ mm). The cylindrical chamber in which the jet is formed has length $x_v = 225$ mm and radius $y_v = 150$ mm, and its initial states are defined by degrees of superheating $R_{p1} = 3.2$ ($p_{c1} = 0.56$ bar) and $R_{p2} = 7$ ($p_{c2} = 0.256$ bar) depending on the experiment.

A two-phase model of a vapor-liquid mixture in the two-temperature, one-pressure, one-velocity approximations, taking into account interphase convective heat transfer and nonequilibrium mass-exchange processes of evaporation and condensation [5], has been developed to solve the problem posed. The system of model equations of conservation of mass, momentum and phase energy used in the numerical implementation is given in the three-dimensional Cartesian coordinate system:

$$\frac{\partial(\alpha_i\rho_i)}{\partial t} + \mathrm{div}\left(\alpha_i\rho_i\mathbf{v}\right) = J_{ij},$$

$$\frac{\partial(\alpha_i\rho_i\mathbf{v})}{\partial t} + \mathrm{div}(\alpha_i\rho_i\mathbf{v}\mathbf{v}) = -\alpha_i\nabla p + \mathrm{div}(\alpha_i\tau_i) + J_{ij}\mathbf{v},$$

$$\frac{\partial(\alpha_i\rho_i E_i)}{\partial t} + \mathrm{div}(\alpha_i\rho_i E_i\mathbf{v}) = -p\frac{\partial\alpha_i}{\partial t} - \mathrm{div}(\alpha_i\mathbf{v}p) + \mathrm{div}(\alpha_i\gamma_{i,eff}\nabla h_i) + K_{ht}(T_j - T_i) + l_s J_{ij}.$$

In the above equations, the following notations have been used: ρ_i — density, T_i — temperature, α_i — volume content, $\mathbf{v}$ — mass velocity vector, J_{ij} — mass transfer rate between i- and j- phases, p — pressure, $\tau_i = \mu_i(\nabla\mathbf{v} + \nabla\mathbf{v}^T) - \frac{2}{3}(\mu_i\mathrm{div}\mathbf{v})\mathrm{I}$ — viscous stress tensor, μ_i — dynamic viscosity, $E_i = e_i + K_i$ — total, internal and kinetic energies, $\gamma_{i,eff}$ — effective diffusivity, h_i — enthalpy, K_{ht} — heat transfer coefficient, l_s — heat of vaporization/condensation. The lower indices $i, j = 1, 2$ correspond to the liquid (l) and gas (g) phases ($i \neq j$).

The thermodynamic properties of the nitrogen gas phase are described by the Peng-Robinson equation of state [6]. The properties of liquid nitrogen by analogy with [7] are

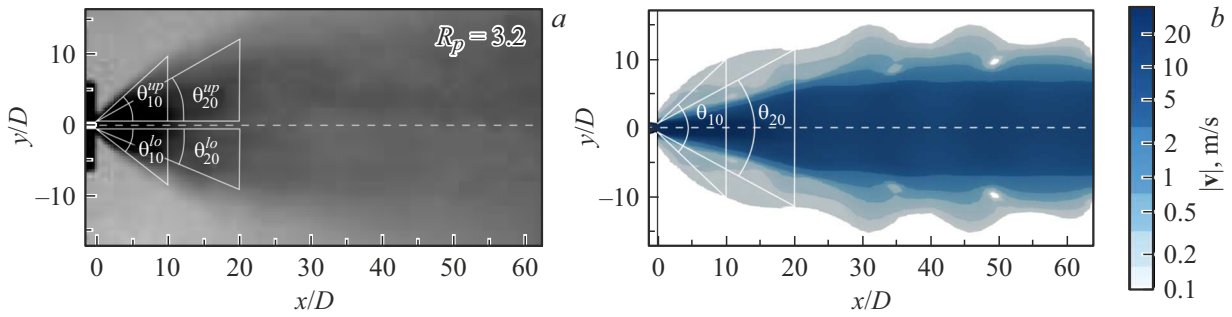

Figure 1. Comparison of the experimental photograph (a) and calculated velocity modulus field distribution (b) with the given schemes for determining the spraying angle [1] for a liquid nitrogen jet at $t = 120$ ms, $R_{p1} = 3.2$, $T_{inj} = 82.5$ K, $p_{inj} = 4$ bar.

determined by the linear equation of state in temperature and density: $\rho = p/(\Gamma c_{VI} T) + \rho_0$, where Γ — the Gruneisen coefficient, which is found by considering the speed of sound $C_l = 780.3$ m/s at pressure $p_s = 1.7$ bar and temperature $T_s = 82.5$ K, and the density ρ_0 corresponds to the state at temperature $T = 0$ K [8,9]. Experimental data for nitrogen [9] at saturation pressure $p_s(T)$ and heat of vaporization $l_s(T)$ are approximated in the form of dependences

$$p_s(T) = p_* \exp\left(-\frac{T_*}{T}\right),$$

$$l_s(T) = l_*\left(\left(\frac{T_{cr}}{T} - 1\right)^{\varphi} - \exp\left(-\frac{T - T_1}{T_2}\right)\right),$$

where $p_* = 7400$ bar, $T_* = 683$ K, $l_* = 2.52 \cdot 10^5$ J/kg, $T_{cr} = 126$ K, $\varphi = 0.31$, $T_1 = 26.5$ K, $T_2 = 20$ K.

The evaporation rate was determined by kinetics [7] as a function of the number n and radius a of the bubbles, saturation temperature $T_s(p)$, heat of vaporization $l_s(T)$, heat transfer coefficient λ_l and Nusselt number Nu: $J_{lg} = 2\pi a n \mathrm{Nu} \lambda_l \big(T - T_s(p)\big)/l_s(T)$.

The model assumes that the phase transition liquid–vapor occurs under non-equilibrium superheated conditions, as in [7] when the temperature of the medium exceeds the saturation temperature: $T > T_s(p) + \Delta T_s$, where ΔT_s — the degree of overheating by temperature. The initial radius of bubbles in liquid nitrogen is given from the characteristic sizes of cavitation nucleation centres [7]: $a = 0.1 \cdot 10^{-6}$ m. At the initial stage of nonequilibrium regime of vapor formation α_g grows due to nucleation of new bubbles on extraneous impurity particles at limited growth of their radius. The number of bubbles at $\alpha_g \leqslant 0.25$ is determined according to [4]: $n = 3\alpha_g/(4\pi a^3)$, $a = 6.5 \cdot 10^{-6}$ m. As the vaporization process develops at $\alpha_g > 0.25$, boiling occurs at a constant number of bubbles due to an increase in their radius: $\alpha_g > 0.25$, $a = \big(3\alpha_g/(4\pi n)\big)^{1/3}$, $n = 4 \cdot 10^{13}$ (in 1 m^3) [4]. The final stage of boiling is characterized by an unrestricted growth of a with the formation of a vapor droplet system with a droplet diameter of $d = 28 \cdot 10^{-6}$ m corresponding to the experimental data [1].

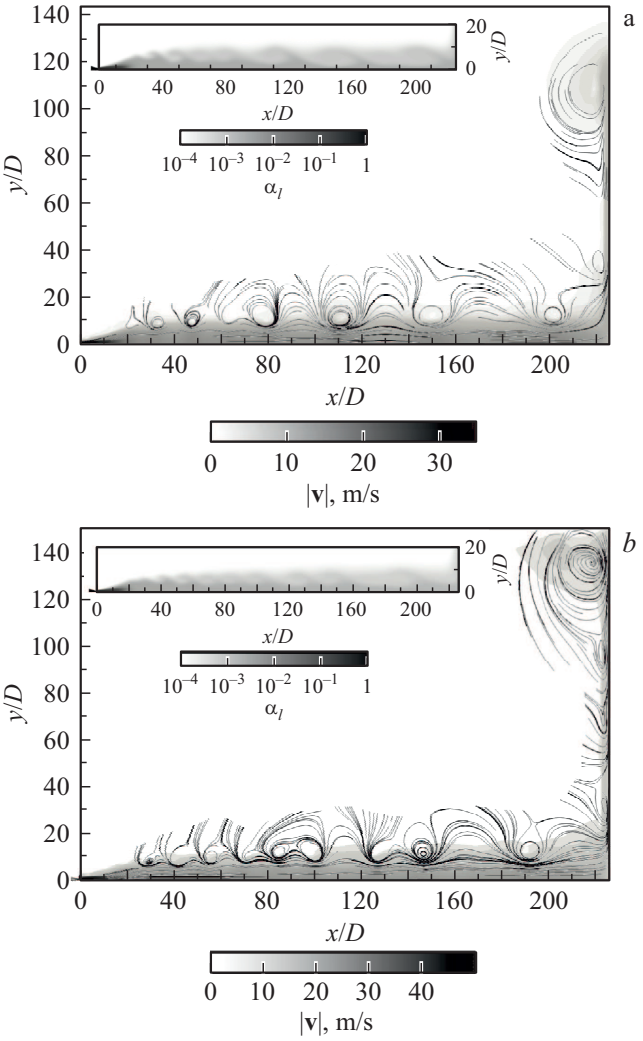

Figure 2. Calculated fields of velocity modulus $|\mathbf{v}(x, y)|$ and streamlines of the boiling nitrogen jet at time $t = 120$ ms at different degrees of superheating. a — $R_{p1} = 3.2$ ($p_{c1} = 0.56$ bar, $T_{inj} = 82.5$ K, $p_{inj} = 4$ bar); b — $R_{p2} = 7$ ($p_{c2} = 0.256$ bar, $T_{inj} = 82.5$ K, $p_{inj} = 4$ bar). The insets — distributions of the volume content of the liquid phase $\alpha_l(x, y)$.

The computer implementation of the proposed vapor-liquid mixture model was carried out using the Open-

FOAM [8] solver developed by the authors. To ensure the accuracy of the numerical solution, the methods of partitioning the mesh domain and time steps were varied. In the best version of the computation used, an adaptive densifying grid consisting of 12 blocks with a total number of cells $\sim 60\,000$. The stability of the solution at the time step in accordance with the Courant condition was achieved at $\Delta t = 1 \cdot 10^{-9}$ s. Approbation of the proposed computational methodology was carried out in [3,4] by comparing numerical solutions with analytical dependences and experimental data.

The validity of the obtained results was evaluated by comparison with the experimental data [1] for the spray angle of the jet at the degree of superheating $R_{p1} = 3.2$ at time $t = 120$ ms after the start of injection as a function of the distance x/D to the nozzle (Fig. 1, *a*). Fig. 1, *a* marks the spray angles at distances $x/D = 10$ and 20 from the nozzle using the scheme proposed in [1]. In the experiment under consideration [1], the values of atomization angles $\theta_{10}^{exp} = (\theta_{10}^{up} + \theta_{10}^{lo})/2 = 80^\circ$ and $\theta_{20}^{exp} = (\theta_{20}^{up} + \theta_{20}^{lo})/2 = 52^\circ$ are given for the indicated distances. Fig. 1, *b* shows the computed velocity modulus fields $|\mathbf{v}(x, y)|$ generated at time $t = 120$ ms of the jet flow and spray angles consistent with experiment [1]: $\theta_{10}^{calc} \approx \theta_{10}^{exp} = 80^\circ$ and $\theta_{20}^{calc} \approx \theta_{20}^{exp} = 52^\circ$.

Figure 2, *a* shows the calculated velocity modulus fields $|\mathbf{v}(x, y)|$ with current lines, the inset shows the liquid phase volume content distribution field $\alpha_l(x, y)$ for the jet formed at time $t = 120$ ms at initial injection conditions $T_{inj} = 82.5$ K and $p_{inj} = 4$ bar for the superheat degree $R_{p1} = 3.2$ at $p_{c1} = 0.56$ bar. In the region bounded by the coordinates $y/D \approx 2$ and $x/D < 50$, the following calculated arithmetic mean values of the mass velocity components in the jet are obtained: $v_x \approx 10$ m/s and $v_y \approx 0.5$ m/s. Fig. 2, *b* shows the calculated distributions of the analyzed jet flow characteristics for the same initial injection conditions as in Fig. 2, *a*, but with a higher degree of superheating $R_{p2} = 7$ ($p_{c2} = 0.256$ bar). The corresponding arithmetic mean values of the velocity components in the above region are $v_x \approx 14$ m/s and $v_y \approx 0.8$ m/s. At the jet axis at $y/D = 0$ and $x/D < 50$, the calculated velocities are equal, respectively: $v_x \approx 30$ m/s in case R_{p1} and $v_x \approx 45$ m/s in case R_{p2}. Starting at time $t > 60$ ms for superheat degree R_{p1} and at $t > 50$ ms for R_{p2} a process of jet reflection from the back surface of the cylindrical low-pressure chamber is formed, which further leads to its sliding along this surface towards the lateral boundary. At the moment $t = 120$ ms in both cases the jet stream reaches the lateral surface, and at higher degree of superheating (Fig. 2, *b*) the reflection process from it starts.

The vortex zones in Fig. 2, *a*, *b*, shown as streamlines, are a consequence of the development of the Kelvin–Helmholtz instability [10], which leads to turbulization of the jet flow with time. An increase in the initial degree of superheating from $R_{p1} = 3.2$ to $R_{p2} = 7$ is accompanied by an increase in the main jet flow velocity from 35 to 50 m/s, which leads to an increase in the angular velocities of vortex formations. Increasing the degree of superheating increases the spray angle of θ_{10}^{calc} from 80 to 102° and θ_{20}^{calc} from 52 to 76°.

Presented in the insets to Fig. 2, *a*, *b* the calculated fields of the liquid nitrogen phase volume content $\alpha_l(x, y)$ showed that a bubble flow region is formed in the near zone at the nozzle exit, where $0.3 \leqslant \alpha_l \leqslant 0.9$ at $0 < x/D < 6$ for $R_{p1} = 3.2$ and at $0 < x/D < 3$ for $R_{p2} = 7$. As the jet moves away from the mouth, it switches to a vapor-drop mode of flow $\alpha_g > 0.9$, and it can be argued that this mode dominates over the bubble mode. When analyzing the distribution of the phase temperature fields, a more marked cooling of the liquid phase in the vapor-drop regime was observed: for $R_{p1} = 3.2$ $T_l \approx 78$ K, and for $R_{p2} = 7$ $T_l \approx 75$ K. The vapor phase cools more intensively along the jet boundary: at $R_{p1} = 3.2$ the temperature values are $T_{gb} \approx 75$ K, and along the symmetry axis $T_{gs} \approx 80$ K. At $R_{p2} = 7$ $T_{gb} \approx 72$ K and $T_{gs} \approx 77$ K. When the jet stream reaches the lateral surface at the jet boundary, the temperature regime is maintained. The phase temperature difference favors the maintenance of a non-equilibrium evaporation regime.

Funding

This study was supported by grant No. 23-29-00309 from the Russian Science Foundation. (https://rscf.ru/en/project/23-29-00309/).

Conflict of interest

The authors declare that they have no conflict of interest.

References

[1] A. Rees, H. Salzmann, J. Sender, M. Oschwald, in *8th Eur. Conf. for aeronautics and space sciences (EUCASS)* (Madrid, Spain, 2019). DOI: 10.13009/EUCASS2019-418

[2] R.Kh. Bolotnova, V.A. Korobchinskaya, E.A. Faizullina, J. Phys.: Conf. Ser., **2103**, 012219 (2021). DOI: 10.1088/1742-6596/2103/1/012219

[3] R.Kh. Bolotnova, V.A. Korobchinskaya, Thermophys. Aeromech., **29** (3), 347 (2022). DOI: 10.1134/S0869864322030039.

[4] R.Kh. Bolotnova, V.A. Korobchinskaya, E.F Gainullina, Lobachevskii J. Math., **44** (5), 1579 (2023). DOI: 10.1134/S1995080223050104

[5] R.I. Nigmatulin, *Dynamics of multiphase media* (Hemisphere, N.Y., 1990).

[6] D.Y. Peng, D.B. Robinson, Ind. Eng. Chem. Fundamen., **15** (1), 59 (1976). DOI: 10.1021/i160057a011

[7] R.H. Bolotnova, V.A. Buzina, M.N. Galimzyanov, V.Sh. Shagapov, Teplofizika i aeromekhanika, **19** (6), 719 (2012).

[8] *OpenFOAM. The Open source computational fluid dynamics (CFD) toolbox* [Electronic source]. http://www.openfoam.com
[9] V.V. Sychev, A.A. Vasserman, A.D. Kozlov, G.A. Spiridonov, V.A. Tsymarny, Termodinamicheskiye svoystva azota (Izdvo Standards, M., 1977).
[10] R. Ishii, H. Fujimoto, N. Hatta, Y. Umeda, J. Fluid Mech, **392**, 129 (1999). DOI: 10.1017/S0022112099005303

Translated by J.Deineka